StarBlocks: Soft Actuated Self-Connecting Blocks for Building Deformable Lattice Structures

Luyang Zhao , Yijia Wu, Wenzhong Yan , Weishu Zhan, Xiaonan Huang , Joran Booth , Ankur Mehta, *Member, IEEE*, Kostas Bekris , *Senior Member, IEEE*, Rebecca Kramer-Bottiglio , and Devin Balkcom

Abstract—In this paper, we present a soft modular block inspired by tensegrity structures that can form load-bearing structures through self-assembly. The block comprises a stellated compliant skeleton, shape memory alloy muscles, and permanent magnet connectors. We classify five deformation primitives for individual blocks: bend, compress, stretch, stand, and shrink, which can be combined across modules to reason about full-lattice deformation. Hierarchical function is abundant in nature and in human-designed systems. Using multiple self-assembled lattices, we demonstrate the formation and actuation of 3-dimensional shapes, including a load-bearing pop-up tent, a self-assembled wheel, a quadruped, a block-based robotic arm with gripper, and non-prehensile manipulation. To our knowledge, this is the first example of active deformable modules (blocks) that can reconfigure into different load-bearing structures on-demand.

Index Terms—Cellular and modular robots, robotics and automation in construction, soft robot materials and design, biologically-inspired robots.
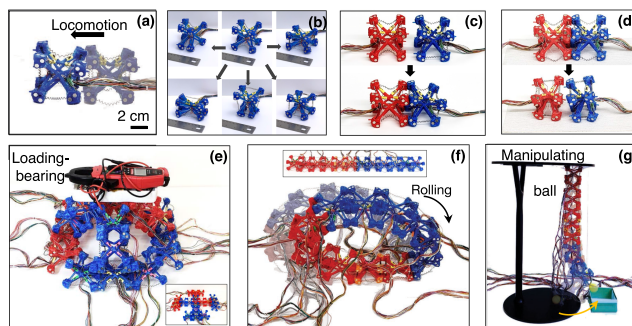

Fig. 1. Starbots: (a) Locomotion of a single module; (b) Five deformation primitives of a single module; (c) Attachment of a pair of modules; (d) Detachment of a pair of modules; (e) Formation and weight-carrying of a 3D dome-shaped tent; (f) Locomotion of a modular rolling robot; (g) Object manipulation of a module-based robotic arm and gripper.

I. INTRODUCTION

IN NATURE, many creatures are capable of working collectively by joining together to form large-scale assemblies to achieve a unified goal, e.g., navigating through unstructured terrain, transporting heavy goods, and surviving in severe environments [1], [2]. For example, the army ants of the *Eciton* genus can use their own bodies to collectively build bridges to span gaps in the colony's foraging trail [3]. The fire ants *Solenopsis*

invicta can form a raft, and can contract their muscles to squeeze the raft into a tight mass to survive a flood [2]. Such collective biological structures are built from individually capable, flexible individuals.

In robotic construction, robotic manipulators often build structures from rigid load-bearing blocks [4], [5], [5], [6], [6], [7], [8], [9], [10], [11], [12], [13], [14], [15], [16], [17], [18]. On the other hand, soft robots can adapt their shapes to suit particular tasks [19], [20], [21]. To bridge the gap between rigid blocks and soft robotics, we design a smart soft modular lattice-based block that can be used for building structures that can deform for locomotion or manipulation, or lock into a shape to bear loads. Individual blocks can locomote, allowing self-assembly into structures without external helpers.

We have previously explored soft modules for locomotion and manipulation [21], but the prior design does not perform as a smart block, as it does not allow 3D lattice stacking or disassembly. The current design also has a much larger deformation space than the previous design; the current design has 12 degrees of actuation compared to 9 for the prior.

There is existing work using rigid *smart blocks*, assembled using a robotic helper [15], [16], [17], [18]. There are also soft *modular* robot designs [22], [23], [24], [25], [26], [27]. However, these soft modular robots do not allow either weight bearing or 3D lattice stacking.

A single module is composed of a stellated skeleton, twelve spring-memory alloy (SMA) actuators, and eight endcaps. SMA variable length tendons [22] are frequently used to actuate soft robots, allowing for limb-like bending when combined with a flexible body. The drawback of SMA is that the current design

does not allow for fast locomotion. Replacing SMA with other actuators like motors would increase the actuation speed. SMA was chosen for its high power density, lightweight, and uniform weight distribution allowing easy attachment to the flexible skeleton.

The core functions of a single block are locomotion, deformation, and connection. To achieve locomotion and deformation primitives, a single module is composed of a soft stellated skeleton printed from Thermoplastic Polyurethane (TPU) material as shown in Fig. 2. At rest, the convex hull of each block is a cube. Twelve SMA actuators connect the vertices of the cube along each of the edges; contraction shortens selected edges, which expand passively when the SMA is relaxed. To enable connection to other blocks, there are eight endcaps at the vertices of the cube, where the same polarity disk magnet is placed in the same position on each endcap. These connections allow blocks to assemble into 3D structures and allows lattices to lock and bear loads. Attachment and detachment between blocks are achieved by the combinations of these core functions, which permits structure self-assembly as well as self-reconfiguration.

We use these capabilities to explore several applications and shapes, with strategies for transformation, locomotion, and manipulation. Specifically, we explored the assembly of a weight-sustaining self-locking tent (Fig. 1(e)), locomotion using both a rolling wheel (Fig. 1(f)) and a quadruped design (Fig. 5(c)), and manipulation using two different strategies: an arm made of modules (Fig. 1(g)), and deformable surface-based peristaltic manipulation (Fig. 5(e)). Further details of these structures appear below in figures 3 and 5. These assemblies are adaptive and compliant, which may make them suitable for unstructured and hazardous environments [28].

Our contribution in this work is to provide a design of a block that can self-assemble with other blocks to create flexible, actuated, load-bearing structures. Self-locomotion, docking, and un-docking properties enable the formation of different structures to achieve various tasks.

II. RELATED WORK

Ground and underwater robotics construction has explored various assembly methods. These methods can be broadly classified into three categories: 1) using an external manipulator to assemble passive blocks [5], [6], [7], [8], [9], [10]; 2) using swarm robots to transport and assemble passive blocks [11], [12], [13], [14]; 3) using programmable blocks with simple robots for structure assembly [15], [16], [17], [18]. Each of these construction methods utilizes rigid blocks with load-bearing capabilities. However, they rely on external assistance for assembly and lack the inherent self-reconfigurability of modular robots.

Modular self-reconfigurable robots (MSRRs) offer a promising alternative approach to traditional construction methods. MSRRs are typically composed of a group of modules, each with the ability to locomote and mechanically join together [29], [30], allowing them to rearrange their connectivity and better adapt to new tasks [31]. Frequently, the individual modules are articulated rigid structures.

Adding compliance and flexibility to modules has been explored as a way to expand the capabilities of soft modular robots [32], [33], including the potential for new modes of actuation and mobility [34], safer interaction with humans [27], and greater adaptation to the physical environment [35]. These soft modular robots can achieve a wide range of morphologies and

functionalities, such as locomotion (e.g. crawling, rolling [19], swimming [36], and cluster-based locomotion [37]), manipulation [24], [38], shape morphology [39], reconfiguration [40], or combinations of these tasks [25], [41]. Nevertheless, most of these soft modular robots rely on manual assembly entirely [19], [25], [34], [36], [38], [39], [40], [41] or initially [20], [23], [37] as their individual modules do not have locomotion capability. None of these soft modular robots are designed for architecture assembly, which means they cannot provide weight-bearing or 3D lattice stacking properties.

III. DESIGN OF A SINGLE BLOCK

Each symmetric block consists of three parts: a soft skeleton, twelve SMA actuators, and eight rigid connectors.

A. Soft Stellated Skeleton and Actuators

The skeleton is rotationally symmetric about different axes in 3D, provides sufficient compliance for various deformation modes, and possesses sufficient space for installing connectors and actuators. Each skeleton resembles a stellated octahedron, with a convex hull that is a cube at rest.

The edge length of each block is $\sim 7.2\,\mathrm{cm}$, and the detwinned Martensite rest length of each SMA (coil diameter, $3.45\,\mathrm{mm}$; wire diameter, $0.51\,\mathrm{mm}$, Dynalloy) is $\sim 3.7\,\mathrm{cm}$. The austenitic (actuated) rest length is $\sim 1.2\,\mathrm{mm}$. When the SMAs are actuated, they are capable of deforming the skeleton, and when the SMAs cool, the skeleton has sufficient restoring force to stretch the SMA back to its detwinned Martensite rest length. We control the SMA open-loop by actuating it for a certain duration under 5 V. We performed physical experiments for each application to determine a suitable actuation duration. The 20% printing fill density and $4\,\mathrm{mm}$ skeleton bar diameter were chosen informed by experiments described in Section V-A. Each SMA coil requires $15-20\,\mathrm{s}$ to cool down and recover from a rigid austenite phase to a relatively compliant martensite phase.

B. Rigid Magnetic Endcap

To limit size, weight, and energy requirements, we chose to use a passive connector with magnets attached. The magnets introduce a trade-off between connection strength and ease of separation. We carefully selected the magnets to provide connection strength while still allowing separation under near-maximum force applied by the SMAs. Experimentally, we found that the magnets with force = 3.566 lbs; diameter = 0.25 inch; thickness = 0.0625 inch matched the selection criteria. The magnetic endcaps consist of two parts: inner endcap (Fig. 2(d) and outer endcap (Fig. 2(e)). The inner endcap is used to connect the skeleton and the outer endcap. Six permanent magnets are mounted on each endcap; two of opposite polarity on each of the three faces. The same polarity disk magnet is placed in the same position on each endcap surface to enable attachment between multiple modules (Fig. 2(e)) [29] to form a lattice structure.

Two additional geometric features are intended to increase connection strength between endcaps as the structure flexes without affecting the separation. One feature is a groove along the diagonal direction. For many flexing motions, this groove prevents sliding motion between endcaps, since magnets provide weak resistance to shear forces. The second feature is that facing endcaps have complementary pegs/holes that further prevent sliding motions.
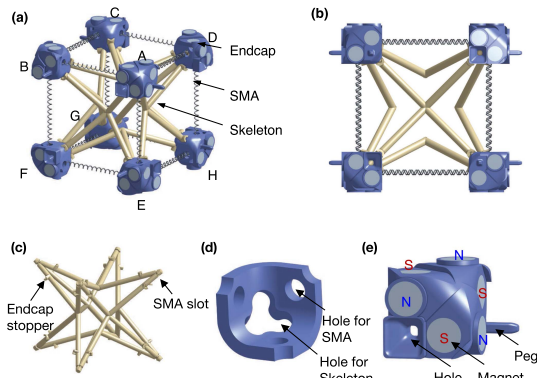
Fig. 2. Module design. (a) A single module is composed of a stellated skeleton, twelve SMA actuators, and eight endcaps. (b) Front/side view of the module. (c) The skeleton is designed to sustain loading and also to hold SMA actuators and endcaps. (d) An endcap's inner part (e) An endcap's outer part.

C. Module Fabrication

The skeleton and endcaps are 3D printed (Voxel 3D Printer, Monoprice) using TPU material (1.75 mm, Amazon Basics) and PETG material (1.75 mm, Amazon Basics) separately. The inner endcaps are glued to the endcap stoppers on the skeleton. Each SMA is crimped with an electric wire and a fishing wire inside a ferrule, and tied to the SMA slot in the skeleton passing through the holes in the inner endcaps. For the outer endcaps, magnets are glued according to the designed polarity as shown in Fig. 2(e). After all the SMAs are assembled, the outer endcaps are glued with the inner endcap. A single module's weight is $47 - 50$ g.

IV. Core Functions of StarBlocks

StarBlocks have three core functions (see Fig. 3), which are *a)* locomotion (to enable self-assembly), *b)* assorted deformation primitives (to enable lattice deformation) *c)* attachment and detachment (to allow formation of shaped lattices).

A. Locomotion

We hand-designed a walking gait that shifts the center of mass (CoM) by increasing the friction/normal force at a planted foot while decreasing the force at the advancing feet by lifting them,similar totensegrity robots [42]. This walking gait enables faster locomotion speed than our previous soft modules could achieve [21]. The detailed locomotion sequence is shown in Fig. 3(a), with the corresponding SMA actuation sequence. The current module design enables a maximum step size that is 89.58% of the body length, which is $\sim 26.15\times$ improvement on our prior work. A module can walk 110 mm in 15 minutes with an average locomotion speed of ~ 7.33 mm/min (0.102 body length/ min), where more than 80% of the time is used for cooling the actuators.

Cost of Transport (COT) is a metric used to evaluate the efficiency of locomotion in robotic systems. COT provides a measure of the energy required to move the robot over a given distance and can be used to compare the efficiency of different locomotion strategies [42]. We calculated the COT for each of our locomotion experiments to provide a quantitative measure of the relative energy efficiency of different assembled structures. We also believe that reporting the COT is important as it allows

other researchers to compare our results to their own and to evaluate the potential real-world applications of our modular robot design. For our system, the COT of single module locomotion is $53200 \ J \cdot m^{-1} \cdot kg^{-1}$. COT values for multi-module structures are provided below.

B. Deformation Primitives

The shape of each module is determined by the lengths of the edges, which can be controlled by the actuation of the corresponding SMAs. In principle, the module can achieve any quadrilaterally-faced hexahedron shape, with some constraints on maximum and minimum size. To simplify control of module shapes and allow reasoning about lattice deformations, we choose five major deformation primitives for a single module: bend, compress, stretch, stand and shrink. Each of these primitives falls into a symmetry class; for example, *stretch* involves two parallel faces (out of six total), so there are three possible stretch actions.

A. Bend allows rotation of one module with respect to another, allowing formation of 3D curved surfaces (see Section VI-A) or rotation actions for locomotion or manipulation (see Section VI-C1). Bend is achieved by actuating two parallel SMAs on one side. The range of the bending angle is from $0°$ to $\sim 30°$.

B. Compress allows linear translation with axial length reduction while increasing the cross-section area. This mode can be used to increase lateral stiffness, which is beneficial for the spatial operation of slender structures (see Section VI-C1). *Compress* is implemented by contracting four parallel SMAs at the same time to reduce the height of the module by $\sim 40\%$.

C. Stretch achieves axial extension while reducing the cross-section area (Fig. 3(b4)). It is obtained by actuating eight SMAs on two opposite surfaces. This mode can be useful for tasks that require axial elongation (see Section VI-B1). The maximum stretching length is $\sim 122\%$.

D. Stand is realized by driving four SMAs on the same surface (Fig. 3(b5)). The area of the corresponding surface becomes smaller with a slight increase of the height This mode can facilitate the generation of curved surfaces by bending four connected modules in different directions and it is useful for detachment of modules (see Section IV-C). We also used this primitive for gripper function (see Section VI-C1).

E. Shrink is implemented by actuating all twelve SMAs simultaneously, the volume is reduced by $\sim 30\%$.

C. Attachment and Detachment Between Modules

Attachment and detachment are needed to form lattices of various shapes. We now describe one effective strategy; others may be possible.

1) Attachment: To attach two modules, one module first remains motionless while the other module approaches. Then, all actuators are turned off and magnetic discs on endcaps form the connection. Due to alignment errors, some of the endcaps may not initially connect. To complete the process and reduce alignment error, both modules simultaneously perform the *stand* primitive to push the modules together. We characterize alignment performance and connection strength in experiments described in Section V.
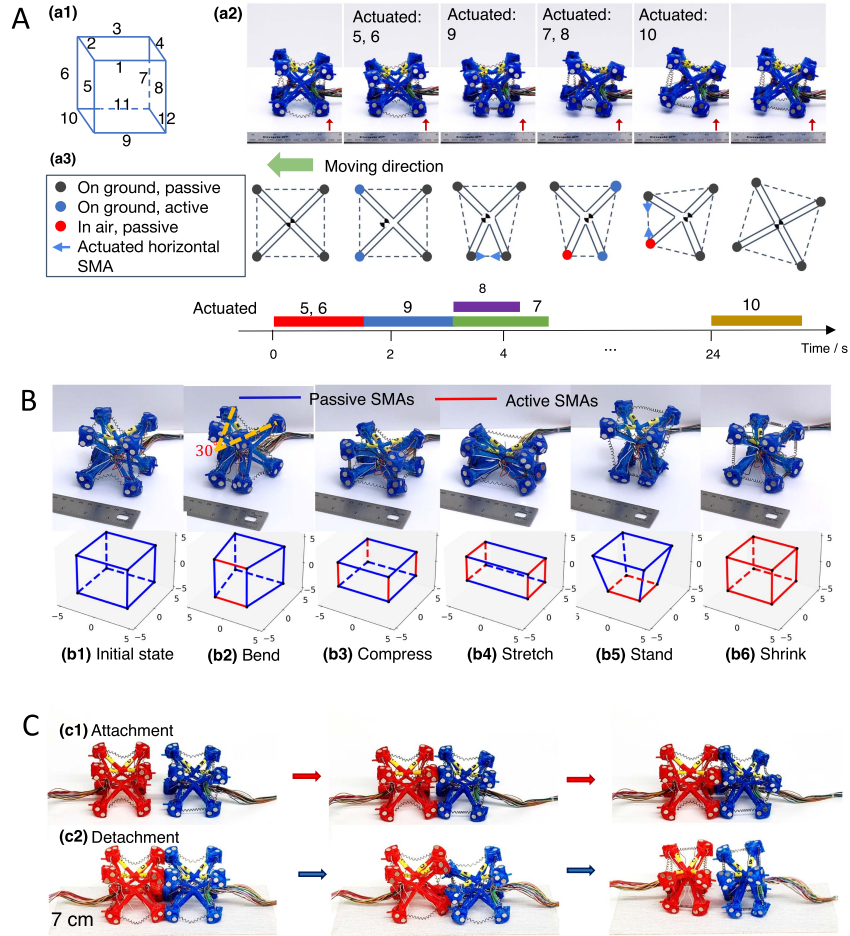
Fig. 3. Core functions. (a) Locomotion of a single block. (a1) A simplified representative of the distribution of SMA actuators with labels; (a2) Snapshots of the locomotion of a block with the corresponding actuated actuators labeled. (a3) top view, timeline, and center of mass location during gait. (b) Deformation primitives of a single block. (c) Attachment and detachment of two blocks.

2) Detachment: To improve the strength of connections, we designed groove and peg-in-a-hole mechanisms. These enhancements, however, make detachment more challenging. Here, we describe one detachment strategy.

The first motion for detachment is a modified "stand" deformation; this deformation introduces large rotation and translation between connected endcaps (Fig. 3(c2)). To create this deformation, vertical SMAs are actuated on one module and horizontal SMAs on the other, along the interface between the modules. After this operation, the coupled endcaps are staggered, but still close to each other. Four SMAs of each module perpendicular to the interface are actuated to pull the endcaps apart. To ensure full detachment, the two modules locomote away from each other. We placed sandpaper on the ground to increase the friction to provide enough force to separate any remaining connections. Without sandpaper, help may be needed from other modules in the lattice; see Fig. 5(b).

V. CHARACTERIZATION EXPERIMENTS

We did experiments to characterize *a)* block stiffness with various rod diameters; *b)* connection force in shear/normal direction with two distinct endcap designs to motivate the peg-in-hole

connector design; *c)* connection success rate between two blocks at varying initial angles and positions.

A. Rod Diameter Choice

Using SMAs, the ideal rod diameter should enable a block *a)* deform into desired shapes when SMAs are actuated and *b)* return to the original shape when SMAs are released.

We did two experiments to find a rod diameter that satisfies both requirements for our particular module geometry. We first tested the relationship between force and displacement of blocks with various diameters. As showed in Fig. 4(a), given the force of four SMAs (the black line) and the displacement we need to achieve (27 mm), only diameters less than 4 mm satisfy the requirement. We then measured the SMA length on each block after release, and found that 4 mm to be an effective rod diameter. We tested the weight capacity of the actuated module and found that it sustained 29.5 N press force. Details are shown by the green line in Fig. 4(a).

B. Connection Force

We did two experiments to measure the normal and shear force using endcaps with/without peg-in-hole designs. Fig. 4(b)
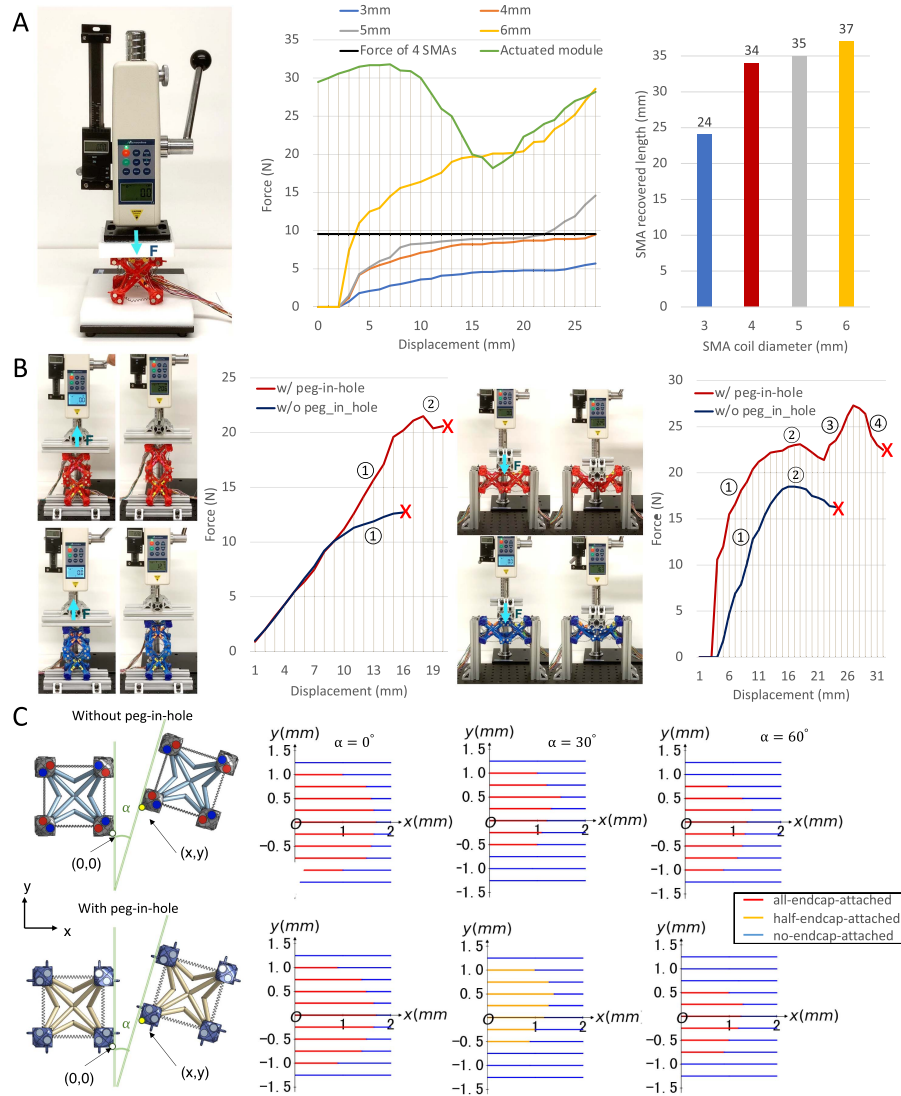
Fig. 4. Characterization experiments for core functions. (a) Relationship between force and displacement of single module with different diameters; SMAs recovered length after cooling down for module with different diameters (b) Characterization experiments for normal force and shear force for blocks w/ and w/o peg-in-hole endcap design. **Left:** ① the force increased until endcaps detached partially (red) or completely (blue) ② force decreased until detaching (red) **Right:** ① Compression force increased until top endcaps detached partially (red & blue) ② force decreased until detached (blue) or the top endcaps touch the bottom endcaps (red) ③ the force needed to compress top and bottom endcaps increased until the bottom endcaps detached partially (red) ④ force decreased until detached (red). (c) Alignment experiments for a pair of modules w/o and w/ peg-in-hole endcap design.

shows the results. The peg-in-hole mechanism is designed to compensate for the weak magnetic strength in the lateral (shear) direction; the joint functions primarily as a mechanical stopper to prevent sliding between endcaps. The two plots show the significant increased force with peg-in-hole design in both directions, allowing larger lattice structures.

C. Alignment

Two blocks will automatically magnetically connect with each other within a certain distance and angle. The relative configuration space is 6D and hard to measure. To simplify, we place both blocks on the ground and fix the position of the left block (showed in Fig. 4(c)), where the right block can move to any position and angles. We discretize the angle into $30°$, $60°$, $90°$, and discretize y value by a step size $= 0.5$ to measure the x values that successfully attach two blocks. In the

experiment, we positioned the right module by hand to achieve a specific initial position and angle. From the experiments, while the peg-in-hole mechanism enlarged the connection force, it also increased the difficulty of alignment. We observe that for 30-degree attachment, only part of the peg-in-hole insertion was achieved for the attached endcaps.

VI. EXAMPLES OF LATTICE STRUCTURES

We provideexamples using StarBlocks to build various lattice structures for construction, manipulation and locomotion.

A. Example of Lattice Structure for Construction

1) Self-Assembly of a Dome-Shaped Tent: A dome-shaped tent formed by StarBlocks demonstrates the capabilities of building load-bearing architecture via self-locking.
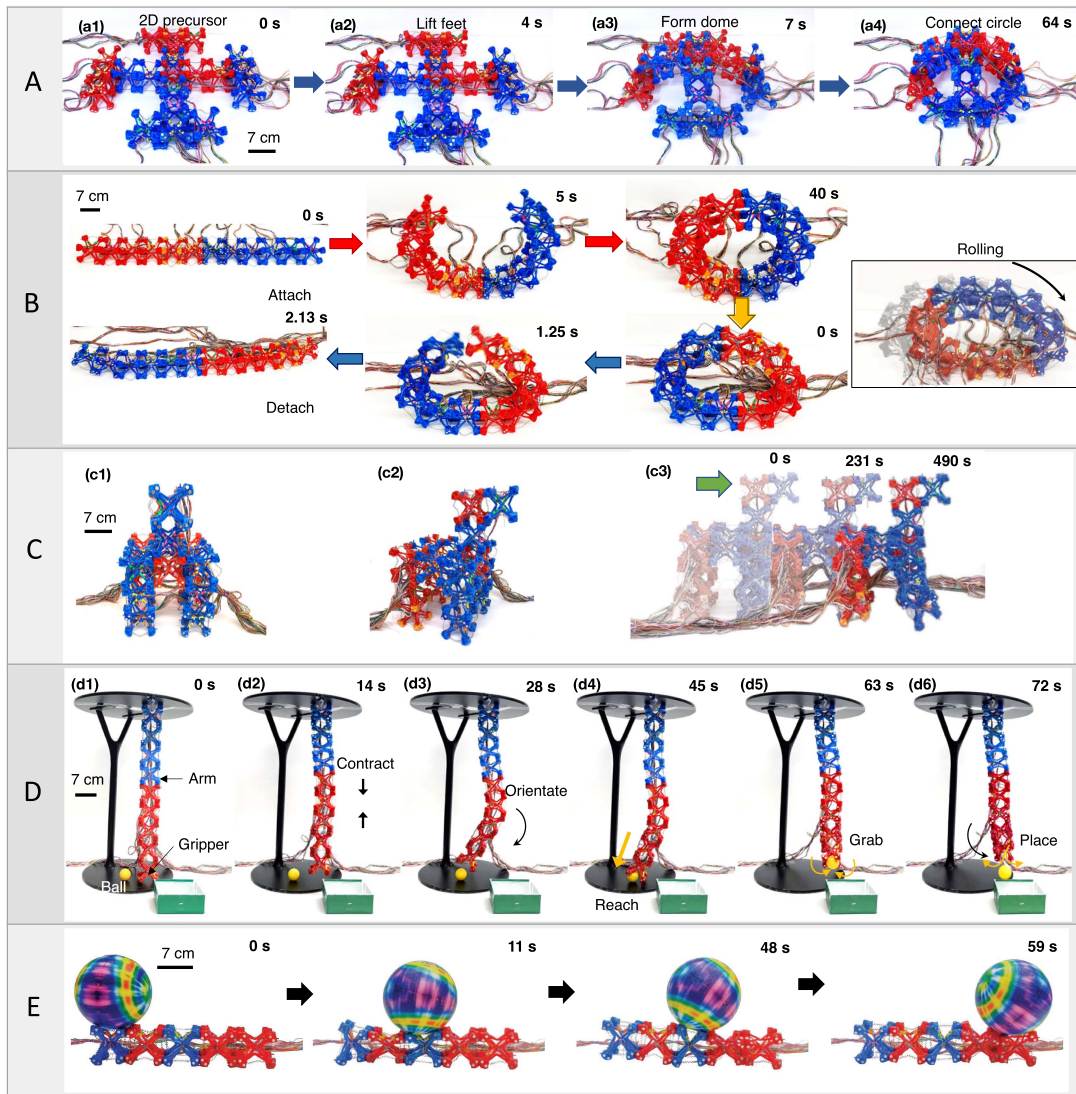
Fig. 5. Applications using StarBlocks. (a) Self-assembly of a dome-shaped tent. (a1) 2D precursor; Snapshots of the formation are shown in (a2)–(a4). (b) Formation and locomotion of a rolling robot. (top left) Self-assembly of the wheel from a chain-shaped precursor to standing wheel; (right) When assembled, the robot can roll forward; the rolling is mainly induced by the shift of center of the mass as modules deform; (bottom left) The rolling robot can self-disassemble back to the chain-shaped configuration by detaching the top-middle connection. (c) Arrangement of modules for a quadruped. (c1) Front view; (c2) Arrangement; (c3) Quadruped with a walking gait. (d) Ball manipulation with a soft robotic arm with a gripper. (d1) Initial state. The tip module functions as a soft gripper; (d2) Lifting up; (d3) Orientating toward the ball; (d4) Stretching to reach; (d5) Grabbing; (d6) Placing the ball into the target box.(e) Non-prehensile manipulation of a ball.

Fig 5(a) shows a 2D precursor shape that can be assembled from loose modules. Modules are arranged into the pattern of a "+" sign with two additional modules at the end of each line segment. "Bend," "stretch," and "stand" modes are then applied by various modules to erect and lock the tent. During tent construction, the central modules arch up to form two orthogonal main arcs of a dome as a supporting skeleton. To realize passive locking and large loading-carry ability after assembly, the additional outer modules passively attach to neighboring modules to form a circle. To simplify the attachment and mediate the alignment issue of neighboring endcaps, we used simplified endcaps without the peg/hole joints for connecting modules.

To verify passive self-locking of the self-assembled tent, we conducted weight load tests without supplied power. The experiment shows that the tent can sustain at most $\sim 1.5\times$ of its own weight (see Fig. 1(e)).

Ultimately, we envision that larger-scale versions of modular deployable tents would be useful for rescue in disasters. Specifically, soft modules can be stored and transported in a compact configuration, and due to their light weight and compliance, and might be dropped into position by helicopter.

B. Example of Lattice Structure for Locomotion

1) Self-Assembly of Rolling Wheel: Fig. 5(b) shows assembly of a chain of modules on plane into a wheel; the rolling process; and the process of disassembly. To assemble the wheel, two ends of a chain of modules attach once the lattice bends. To roll the wheel, the center of mass of the wheel is shifted rightwards continuously, by repeatedly stretching the module close to the bottom labeled in Fig. 6. Currently, the wheel can move forward 72 mm in 52 s, achieving an average speed of ~ 82.8 mm/min
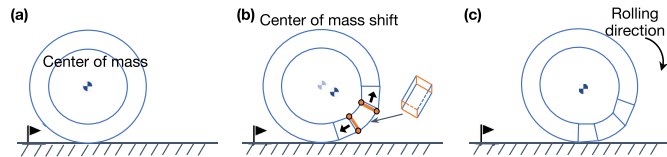
Fig. 6. Locomotion mechanism of the rolling robot. (a) Initially, the center of the mass is in the middle; (b) The center of the mass shifts rightward when we stretch the specific module; (c) The shift causes the robot to roll forward.

Fig. 7. Maximum reach of the arm in the x direction; black dots show a point on the center of the end effector.

(1.15 body length/ min), which is $11\times$ the maximum speed of the gaits we developed for a single module. The locomotion could be sped up by reducing the cooling time needed for SMAs [21]. The Cost of Transport (COT) is $4782\,\mathrm{J}\cdot\mathrm{m}^{-1}\cdot\mathrm{kg}^{-1}$. To disassemble the wheel, we use the detachment strategy to separate any two modules on the top of the wheel. With the help of the gravity of adjacent modules, the two modules on the top separate easily.

2) Quadruped Dog Locomotion: To explore multi-legged gaits, we manually assembled 19 blocks together to form a dog-inspired quadruped (Fig. 5(c)), since we do not yet have a strategy for vertical assembly. Each leg is composed of two blocks, with an eight-block body and a three-block head.

There are different gaits that a real dog uses for locomotion, where trot is the most efficient pattern [43]. For the "Trot" pattern, two legs on the diagonal move forward together. For our case, to simplify, we modified the normal "Trot" pattern and instead of letting two diagonal feet move at the same time, we move the rear foot first to permit a longer time for landing. In particular, we loop over the pattern "left-rear $\rightarrow$ right-front $\rightarrow$ release-SMAs $\rightarrow$ right-rear $\rightarrow$ left-front $\rightarrow$ release-SMAs". This arrangement of blocks can locomote $730\,\mathrm{mm}$ in 10.4 minutes with an average speed of $\sim 70.19\,\mathrm{mm/min}$ (0.975 body length/ min), which is ~ 9.58 times the speed of the single block and 77% of the time is used in releasing the SMA actuators; the COT is $898\,\mathrm{J}\cdot\mathrm{m}^{-1}\cdot\mathrm{kg}^{-1}$, which is the most energy-efficient locomotion method in this paper. For comparison, Huang et al. [44] designed a soft robot actuated by SMA, and the calculated COT equal to $786\,\mathrm{J}\cdot\mathrm{m}^{-1}\cdot\mathrm{kg}^{-1}$.

C. Examples of Lattice Structure for Manipulation

In this section, we explore two very different strategies for object manipulation: an arm-based gripper, and non-prehensile contact juggling along the surface of the lattice.

1) Module-Based Gripper and Robot Arm: We implemented a block-based robot arm to grasp objects and deliver them to a target box. We designed three control strategies for the arm. a) "lift:" uses "compress" primitives vertically to decrease the vertical length of robot arm. b) "extend:" uses "stretch" primitives vertically to increase the length of the arm. c) "re-orient:" individual modules use "bend" primitives.

To perform the experiments, we mounted a chain of modules under a round table as Fig. 5(d)) shows. We used a single module as a gripper to grasp an object with the "stand" primitive. The payload capacity of the arm depends on the connection force between the uppermost module and the second uppermost module as it endures the load and the gravity of all the modules below the uppermost module.

Our experiments in Section V-B demonstrate the endcaps can sustain more than 20 N before detachment. Considering the estimated gravity of the eight modules attached below the top

module as 4 N, the arm's maximum payload in fully extended configuration is no greater than $16\,\mathrm{N}/1.6\,\mathrm{kg}$.

We also did an experiment to measure some characteristics of the workspace. We found the maximum reach in the x direction is around $26\,\mathrm{cm}$, and the maximum height the effector can be lifted is roughly $25.5\,\mathrm{cm}$ (shown in Fig. 7).

Similar to other soft arms, the benefits of the arm structure we explored are that it is flexible, has high error tolerance and provides safe human-robot interaction. Furthermore, we imagine that the module-based arm and gripper could reconfigure into other shapes for objects with different shapes and weights. For example, to grasp larger objects, modules might be re-arranged into other shapes, such as using five modules to form the gripper in the shape of an inverted letter U.

2) Non-Prehensile Manipulation: Fig. 5(e) shows linear manipulation using assembled blocks. The principal is to create a wave-like surface deformation to transport the objects similar to what we implemented in prior work [21].

VII. CONCLUSION AND FUTURE WORK

In this letter, we designed a soft robotic block that can build passive weight-sustaining structures or actuated structures for locomotion and manipulation. Self-locomotion and deformation primitives, as well as attachment/detachment capabilities, permit behaviors including self-reconfiguration, self-assembly, complex deformation, and robust locomotion.

The proposed system provides opportunities for additional design and development. Un-tethered robots are needed for deployment outside of the lab, requiring on-board power, computing, sensors, and inter-block communications. To enable better reconfiguration, we would like to close the loop by adding an external sensor. Other actuators, such as electromagnetic motors, dielectric elastomer actuators [45], or super-coiled polymer actuators [46], would increase actuation speed, with mass or strength trade-offs.

Our system is capable of self-assembly and self-disassembly using unique endcaps with magnets. While the mechanical design of endcaps increases the connection force between modules, the configuration space of alignment also decreased. To completely detach two modules, helper modules, external forces, or sandpaper are currently needed due to the strength of the magnetic force. New designs are necessary to improve self-disassembly, such as adding actuators to increase the distance between magnets to decrease the magnetic force [47] or using an electromagnet. Another limitation of the current connector is that the limited connection strength limits the scale of lattices and their range of motion. We are exploring new, stronger connector designs.

Each of the applications (e.g., tent, wheel, arm) show different potentials, but need refinement to be practically useful. For example, the tent deployment relies on low friction and a smooth ground surface. The single-chain wheel exhibits distinct locomotion capability, but is not particularly stable. A double wheel might provide such stability. The module-based arm provides high deformation, but limitations of the connectors limit the weight of the objects that it can manipulate.

References

[1] C. Anderson, G. Theraulaz, and J.-L. Deneubourg, "Self-assemblages in insect societies," *Insectes Sociaux*, vol. 49, no. 2, pp. 99–110, 2002.

[2] S. Murata and H. Kurokawa, *Self-Organizing Robots*, vol. 77. New York, NY, USA: Springer, 2012.

[3] C. R. Reid, M. J. Lutz, S. Powell, A. B. Kao, I. D. Couzin, and S. Garnier, "Army ants dynamically adjust living bridges in response to a cost–benefit trade-off," *Proc. Nat. Acad. Sci.*, vol. 112, no. 49, pp. 15113–15118, 2015.

[4] K. S. Saidi, T. Bock, and C. Georgoulas, "Robotics in construction," in *Springer Handbook of Robotics*. Cham, Switzerland: Springer, 2016, pp. 1493–1520.

[5] B. Jenett, A. Abdel-Rahman, K. Cheung, and N. Gershenfeld, "Material–robot system for assembly of discrete cellular structures," *IEEE Robot. Automat. Lett.*, vol. 4, no. 4, pp. 4019–4026, Oct. 2019.

[6] N. B. Cramer et al., "Elastic shape morphing of ultralight structures by programmable assembly," *Smart Mater. Structures*, vol. 28, no. 5, Apr. 2019, Art. no. 055006.

[7] M. Saboia, V. Thangavelu, and N. Napp, "Autonomous multi-material construction with a heterogeneous robot team," in *Robotics and Autonomous Systems.*. New York, NY, USA: Springer, 2019, pp. 385–399.

[8] K. Dörfler, T. Sandy, M. Giftthaler, F. Gramazio, M. Kohler, and J. Buchli, "Mobile robotic brickwork," in *Robotic Fabrication in Architecture, Art and Design 2016*. New York, NY, USA: Springer, 2016, pp. 204–217.

[9] E. Gambao, C. Balaguer, A. Barrientos, R. Saltaren, and E. A. Puente, "Robot assembly system for the construction process automation," in *Proc. Int. Conf. Robot. Automat.*, 1997, vol. 1, pp. 46–51.

[10] S. Lensgraf et al., "Droplet: Towards autonomous underwater assembly of modular structures," in *Proc. Robot.: Sci. Syst.*, 2021.

[11] J. Werfel, *Building Blocks for Multi-Robot Construction*. New York, NY, USA: Springer, 2004.

[12] Y. Terada and S. Murata, "Automatic modular assembly system and its distributed control," in *Int. J. Robot. Res.*, vol. 27, no. 3–4, pp. 445–462, 2008.

[13] T. Wareham and A. Vardy, "Putting it together: The computational complexity of designing robot controllers and environments for distributed construction," *Swarm Intell.*, vol. 12, no. 2, pp. 111–128, 2018.

[14] M. K. Heinrich et al., "Using interactive evolution to design behaviors for non-deterministic self-organized construction," in *Proc. Symp. Simul. Architecture Urban Des.*, 2018.

[15] K. Sugawara and Y. Doi, "Collective construction of dynamic structure initiated by semi-active blocks," in *Proc. IEEE/RSJ Int. Conf. Intell. Robots Syst.*, 2015, pp. 428–433.

[16] J. Werfel, Y. Bar-Yam, D. Rus, and R. Nagpal, "Distributed construction by mobile robots with enhanced building blocks," in *Proc. IEEE Int. Conf. Robot. Automat.*, 2006, pp. 2787–2794.

[17] J. Werfel, "Collective construction with robot swarms," in *Morphogenetic Engineering*. New York, NY, USA: Springer, 2012, pp. 115–140.

[18] B. Piranda and J. Bourgeois, "Designing a quasi-spherical module for a huge modular robot to create programmable matter," *Auton. Robots Volume,* vol. 42, pp. 1–15, 2018.

[19] C. D. Onal and D. Rus, "A modular approach to soft robots," in *Proc. IEEE 4th RAS EMBS Int. Conf. Biomed. Robot. Biomechatronics*, 2012, pp. 1038–1045.

[20] A. Vergara, Y.-S. Lau, R.-F. Mendoza-Garcia, and J. C. Zagal, "Soft modular robotic cubes: Toward replicating morphogenetic movements of the embryo," *PLoS One*, vol. 12, no. 1, Jan. 2017, Art. no. e0169179.

[21] L. Zhao et al., "Soft lattice modules that behave independently and collectively," *IEEE Robot. Automat. Lett.*, vol. 7, no. 3, pp. 5942–5949, Jul. 2022.

[22] C. Lee et al., "Soft robot review," *Int. J. Control, Automat. Syst.*, vol. 15, pp. 3–15, 2017.

[23] J. Zou, Y. Lin, C. Ji, and H. Yang, "A reconfigurable omnidirectional soft robot based on caterpillar locomotion," *Soft Robot.*, vol. 5, no. 2, pp. 164–174, Apr. 2018.

[24] R. M. McKenzie, M. E. Sayed, M. P. Nemitz, B. W. Flynn, and A. A. Stokes, "Linbots: Soft modular robots utilizing voice coils," *Soft Robot.*, vol. 6, no. 2, pp. 195–205, 2019.

[25] S. W. Kwok et al., "Magnetic assembly of soft robots with hard components," *Adv. Funct. Mater.*, vol. 24, no. 15, pp. 2180–2187, 2014.

[26] S. Li and D. Rus, "Jellocube: A continuously jumping robot with soft body," *IEEE/ASME Trans. Mechatron.*, vol. 24, no. 2, pp. 447–458, Apr. 2019.

[27] N. S. Usevitch, Z. M. Hammond, M. Schwager, A. M. Okamura, E. W. Hawkes, and S. Follmer, "An untethered isoperimetric soft robot," *Sci. Robot.*, vol. 5, no. 40, 2020, Art. no. eaaz0492.

[28] L. Pfotzer, S. Ruehl, G. Heppner, A. Roennau, and R. Dillmann, "Kairo 3: A modular reconfigurable robot for search and rescue field missions," in *Proc. IEEE Int. Conf. Robot. Biomimetics*, 2014, pp. 205–210.

[29] J. W. Romanishin, K. Gilpin, and D. Rus, "M-blocks: Momentum-driven, magnetic modular robots," in *Proc. IEEE/RSJ Int. Conf. Intell. Robots Syst.*, 2013, pp. 4288–4295.

[30] "Roombots extended: Challenges in the next generation of self-reconfigurable modular robots and their application in adaptive and assistive furniture," *Robot. Auton. Syst.*, vol. 127, 2020, Art. no. 103467.

[31] M. Yim et al., "Modular self-reconfigurable robot systems [grand challenges of robotics]," *IEEE Robot. Automat. Mag.*, vol. 14, no. 1, pp. 43–52, Mar. 2007.

[32] C. Zhang, P. Zhu, Y. Lin, Z. Jiao, and J. Zou, "Modular soft robotics: Modular units, connection mechanisms, and applications," *Adv. Intell. Syst.*, vol. 2, 2020, Art. no. 1900166.

[33] D. Zappetti, S. Mintchev, J. Shintake, and D. Floreano, "Bio-inspired tensegrity soft modular robots," in *Proc. Conf. Biomimetic Biohybrid Syst.*, 2017, pp. 497–508.

[34] J.-Y. Lee, W.-B. Kim, W.-Y. Choi, and K.-J. Cho, "Soft robotic blocks: Introducing SoBL, a fast-build modularized design block," *IEEE Robot. Automat. Mag.*, vol. 23, no. 3, pp. 30–41, Sep. 2016.

[35] Y. Ozkan-Aydin and D. I. Goldman, "Self-reconfigurable multilegged robot swarms collectively accomplish challenging terradynamic tasks," *Sci. Robot.*, vol. 6, no. 56, 2021, Art. no. eabf1628.

[36] S. Mintchev et al., "An underwater reconfigurable robot with bioinspired electric sense," in *Proc. IEEE Int. Conf. Robot. Automat.*, 2012, pp. 1149–1154.

[37] S. Ceron, M. A. Kimmel, A. Nilles, and K. Petersen, "Soft robotic oscillators with strain-based coordination," *IEEE Robot. Automat. Lett.*, vol. 6, no. 4, pp. 7557–7563, Oct. 2021.

[38] S. Kurumaya et al., "A modular soft robotic wrist for underwater manipulation," *Soft Robot.*, vol. 5, no. 4, pp. 399–409, 2018.

[39] Q. Ze et al., "Soft robotic origami crawler," *Sci. Adv.*, vol. 8, no. 13, 2022, Art. no. eabm7834.

[40] S. Li et al., "Scaling up soft robotics: A meter-scale, modular, and reconfigurable soft robotic system," *Soft Robot.*, vol. 9, no. 2, pp. 324–336, 2022.

[41] M. A. Robertson and J. Paik, "New soft robots really suck: Vacuum-powered systems empower diverse capabilities," *Sci. Robot.*, vol. 2, no. 9, 2017, Art. no. eaan6357.

[42] D. S. Shah et al., "Tensegrity robotics," *Soft Robot.*, vol. 9, no. 4, pp. 639–656, 2022.

[43] B. J. Carr and D. Dycus, "Canine gait analysis," *Today's Veterinary Practice*, vol. 6, no. 2, pp. 93–98, 2016.

[44] X. Huang, K. Kumar, M. K. Jawed, Z. Ye, and C. Majidi, "Soft electrically actuated quadruped (SEAQ)–integrating a flex circuit board and elastomeric limbs for versatile mobility," *IEEE Robot. Automat. Lett.*, vol. 4, no. 3, pp. 2415–2422, Jul. 2019.

[45] X. Ji et al., "An autonomous untethered fast soft robotic insect driven by low-voltage dielectric elastomer actuators," *Sci. Robot.*, vol. 4, no. 37, 2019, Art. no. eaaz6451.

[46] W. Yan and A. Mehta, "A cut-and-foldself-sustained compliant oscillator for autonomous actuation of origami-inspired robots," *Soft Robot.*, vol. 9, no. 5, pp. 871–881, 2022.

[47] B. S. Smith, F. C. Simeone, A. A. Stokes, and G. M. Whitesides, "Magnetic assembly of soft robots with hard components," *Adv. Funct. Mater.*, vol. 24, no. 15, pp. 2180–2187, 2014.